
Proceedings Paper:
McAree, O., Aitken, J.M. orcid.org/0000-0003-4204-4020 and Veres, S.M. (2017) Towards artificial situation awareness by autonomous vehicles. In: IFAC-PapersOnLine. 20th IFAC World Congress, 09/07/2017 - 14/07/2017, Toulouse, France. Elsevier , pp. 7038-7043.

https://doi.org/10.1016/j.ifacol.2017.08.1349

Towards artificial situation awareness by autonomous vehicles ⋆

Owen McAree * **Jonathan M. Aitken** * **Sandor M. Veres** *

* *Department of Automatic Control and Systems Engineering, University of Sheffield, UK (e-mail: o.mcaree, jonathan.aitken, s.veres@sheffield.ac.uk).*

Abstract: This paper presents a novel approach to artificial situation awareness for an autonomous vehicle operating in complex dynamic environments populated by other agents. A key aspect of situation awareness is the use of mental models to predict future states of the environment, allowing safe and rational routing decisions to be made. We present a technique for predicting future discrete state transitions (such as the commencement of a turn) by other agents, based upon an uncertain mental model. Predictions take the form of univariate Gaussian Probability Density Functions which capture the inherent uncertainty in transition time whilst still providing great benefit to a decision making system. The prediction distributions are compared with Monte Carlo simulations and show an excellent correlation over long prediction horizons.

Keywords: Autonomous systems, Decision making and autonomy, Navigation, Safety, Human and vehicle interaction

1. INTRODUCTION

Autonomous vehicles operating in complex environments, particularly those in close proximity to human agents [1], are required to make safe, rational decisions about how they behave. These decisions should also be made in a manner which is analogous to those made by human agents, so they may be easily understood by them (Hutchings et al., 2007; Chen et al., 2015). This leads to a requirement for the autonomous agent to possess a high level of situation awareness, defined by Endsley (1988) as the ability to predict future states of the environment based upon a perception of the current state and a comprehension of its meaning. This prediction step is based on a mental model of the environment, including other agents, and enables the autonomous agent to make decisions, which are not only safe at the current time, but will likely continue to be safe in the future (Endsley, 1995; Adams, 2007).

McAree (2013) introduced this concept of artificial situation awareness by considering an autonomous Unmanned Aircraft System (UAS) landing at a busy airfield at which manned vehicles were also landing. The mental model of the traffic behaviour consist of both continuous and discrete elements

(1) Continuous - Velocity, rate of turn and heading uncertainty
(2) Discrete - Changes in the route of the vehicle due to local air traffic procedures

Parameters of the models may be uncertain, and are represented as univariate Gaussian distributions which can be easily constructed from observed data, such as radar traces (Bar-Shalom and Li, 1993).

McAree and Chen (2013) predicted future positions of traffic as two dimensional spatial Probability Density Functions (PDFs), before computing a separation distribution as a univariate PDF. The possibility of discrete transitions invalidates the often used constant velocity assumption (Livadas et al., 2000; Pellegrini et al., 2009; Winfield et al., 2014), therefore the intermediate spatial PDF becomes highly non-Gaussian and requires the use of dense non-parametric models to correctly capture the uncertainty (McAree, 2013). Despite this non-Gaussianity, the final separation PDF can be closely approximated to a Gaussian, albeit requiring significant computational power.

In this paper, we propose an abstraction which transforms the prediction problem from the two dimensional spatial domain to the one dimensional temporal domain. Rather than attempting to predict future positions of other agents directly, we seek to predict the time at which future discrete transitions will occur, as a univariate PDF. This approach significantly reduces the computational burden of future state prediction, without significant loss in utility. For example, if an autonomous car observes another vehicle approaching a roundabout it need not be concerned with the future latitude and longitude of the traffic, only if it is likely to be on the roundabout at the same time as itself. The next section presents the principle behind discrete transition prediction for simple scenarios where spacial uncertainty is bounded, including the aforementioned roundabout scenario as a numerical example.

Neglecting to perform any prediction of spatial uncertainty may be computationally desirable, but it leads to significant errors in temporal prediction for complex environments with unbounded uncertainty, such as in the UAS

⋆ Research in part supported by the EPSRC, grant numbers EP/L024942/1 and EP/J011843/1

[1] Either people, or manually controlled vehicles

example mentioned previously. Section 3 builds on the simple case by considering spatial uncertainty only so far as it pertains to temporal uncertainty, and uses the same UAS example to explain the necessary calculation steps.

Section 4 introduces situations where the list of future discrete transitions may not be known precisely, and how these probabilities can be inferred from observation along with the online learning of mental models.

Finally, Section 5 concludes this work and discusses links to future work on agent decision making, learning and verification.

2. SIMPLE TEMPORAL SITUATION AWARENESS

In domains where spatial uncertainty is limited by the environment, and the required prediction horizons are relatively short, it is possible to determine transition PDFs directly from transit and manoeuvre time distributions. In two dimensions we define transit time as the time taken to travel a particular, although possible uncertain, distance. Manoeuvre time is defined as the time taken to turn through a particular, although possibly uncertain, angle. In simple scenarios these two concepts are mathematically very similar, however they are dealt with separately to facilitate the extension to complex scenarios in the next section.

2.1 Transit time distribution

Transit time is defined as the time taken to travel a particular distance at a particular speed. If these were both known with certainty the calculation would be trivial, however if $v \sim \mathcal{N}(\bar{v}, \tilde{v}^2)$ and $d \sim \mathcal{N}(\bar{d}, \tilde{d}^2)$ then $t_t = d/v$ is a ratio distribution which in general is undefined (Hayya et al., 1975). Under certain restrictions, however, it is possible to approximate the distribution t_t to a Gaussian.

Lemma 1. Given the uncorrelated Gaussian distributions $x \sim \mathcal{N}(\bar{x}, \tilde{x}^2)$ and $y \sim \mathcal{N}(\bar{y}, \tilde{y}^2)$, the distribution $z = y/x$ can be approximated to $z \sim \mathcal{N}(\bar{z}, \tilde{z}^2)$, where $\bar{z} = \bar{y}/\bar{x}$ and $\tilde{z}^2 = (\tilde{x}\bar{y}/\bar{x}^2)^2 + (\tilde{y}/\bar{x})^2$. Provided $\bar{x} > 0$, $\bar{y} > 0$ and $\tilde{x} \ll \bar{x}$.

Proof. As x and y are uncorrelated we consider their contributions to z as having mean $\bar{z} = \bar{y}/\bar{x}$ and variance found from the convolution of the two independent distributions $z_x = \bar{y}/x$ and $z_y = y/\bar{x}$ as

$$\tilde{z}^2 = \tilde{z}_x^2 + \tilde{z}_y^2 \tag{1}$$

z_y is simply an affine transform of y, therefore $\tilde{z_y} = \tilde{y}/\bar{x}$

z_x is generally undefined (Seshadri, 1993), but can be approximated by taking the exponent of the Gaussian PDF for x, substituting $x = \bar{y}/z_x$, and rearranging to the standard form, leading to

$$\bar{z}_x = \frac{\bar{y}}{\bar{x}} \tag{2}$$

$$\tilde{z}_x = \frac{\tilde{x} z_x}{\bar{x}} \tag{3}$$

Equation (2) is the expected mean, however, (3) does not represent a valid variance, as it is a function of the random variable z_x. By writing $z_x = \bar{z}_x + \tilde{z}_x\sigma$, where $\sigma \sim \mathcal{N}(0, 1)$

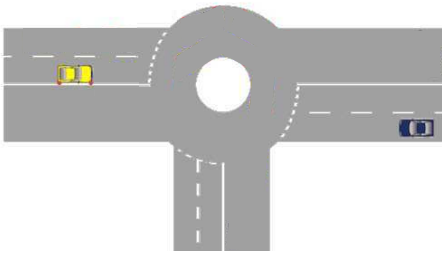

Fig. 1. Example: traffic vehicle (left) intending to cross path of autonomous vehicle (right)

and assuming $\tilde{z}_x \ll \bar{z}_x$ (therefore the $\tilde{z}_x\sigma$ term may be neglected as small), we can find that

$$\tilde{z}_x = \frac{\tilde{x}\bar{y}}{\bar{x}^2} \tag{4}$$

The condition to satisfy $\tilde{z} \ll \bar{z}$ can be found from (2) and (4) as $\tilde{x} \ll \bar{x}$ □

Corollary 2. Given a Gaussian velocity distribution $v \sim \mathcal{N}(\bar{v}, \tilde{v})$, the time taken to travel a distance $d \sim \mathcal{N}(\bar{d}, \tilde{d})$ can be approximated to the distribution $t_t \sim \mathcal{N}(\bar{t}_t, \tilde{t}_t^2)$, where $\bar{t}_t = \bar{d}/\bar{v}$ and $\tilde{t}_t^2 = (\tilde{v}\bar{d}/\bar{v}^2)^2 + (\tilde{d}/\bar{v})^2$. Provided $\tilde{v} \ll \bar{v}$.

Proof. Travel time is defined as $t_t = d/v$, where $\bar{v} > 0$ and $\bar{d} > 0$. d and v can be considered independent as the uncertainty in the speed and distance to be travelled do not effect one another. The result follows Lemma 1. □

2.2 Manoeuvre time distribution

A manoeuvre is defined as rotation through a particular angle ψ at a particular angular rate $\dot{\psi}$, both of which can be uncertain. In the simple case where spatial uncertainty is limited and prediction horizons are small the manoeuvre time distribution is found in an identical way to the transit time above. Generally

$$t_m \sim \mathcal{N}(\bar{t}_m, \tilde{t}_m^2) \tag{5}$$

where $\bar{t}_m = \bar{\psi}/\bar{\dot{\psi}}$ and $\tilde{t}_m^2 = (\tilde{\psi}\bar{\psi}/\bar{\dot{\psi}}^2)^2 + (\tilde{\psi}/\bar{\dot{\psi}})^2$

2.3 Automotive example

To illustrate the use of the transit and manoeuvre time distributions for predicting discrete state transitions, consider an autonomous car detecting an oncoming vehicle which is signalling to cross its path at a roundabout, Fig. 1. This example contains four discrete states of interest

(1) Transit from currently observed position to roundabout, where both the distance and velocity are uncertain. $d_1 \sim \mathcal{N}(50m, (0.25m)^2)$ and $v_1 \sim \mathcal{N}(15ms^{-1}, (1ms^{-1})^2)$
(2) Left turn to enter the roundabout, where turn rate is uncertain. $\dot{\psi}_2 \sim \mathcal{N}(45^o s^{-1}, (2^o s^{-1})^2)$
(3) Right turn on roundabout, where turn rate is uncertain. $\dot{\psi}_3 \sim \mathcal{N}(45^o s^{-1}, (2^o s^{-1})^2)$
(4) Left turn to exit roundabout, where turn rate is uncertain. $\dot{\psi}_4 \sim \mathcal{N}(45^o s^{-1}, (2^o s^{-1})^2)$

Fig. 2 illustrates 10,000 potential trajectories for the traffic vehicle which is initially located at $(0, 0)m$. Applying Corollary 2 to the first state and (5) to the rest yields

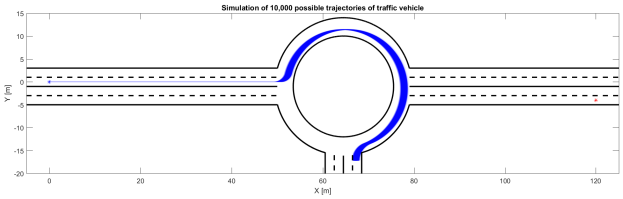

Fig. 2. Monte-carlo experiment of 10,000 executions

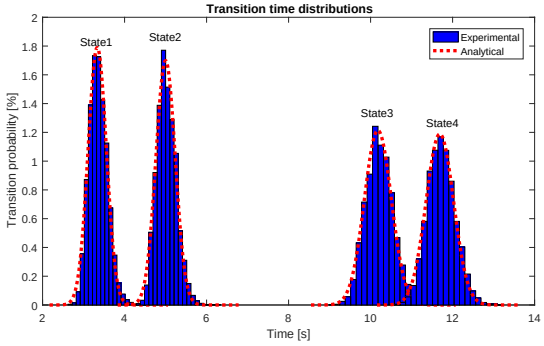

Fig. 3. Experimental and analytical transitions probabilities

$$t_{0,1} \sim \mathcal{N}(3.33s, (0.223s)^2) \quad (6)$$
$$t_{1,2} \sim \mathcal{N}(1.67s, (0.074s)^2) \quad (7)$$
$$t_{2,3} \sim \mathcal{N}(5.18s, (0.230s)^2) \quad (8)$$
$$t_{3,4} \sim \mathcal{N}(1.51s, (0.070s)^2) \quad (9)$$

Calculation of the transitions times is simply the cumulative convolution of these individual distributions

$$t_1 = t_{0,1} \sim \mathcal{N}(3.33s, (0.223s)^2) \quad (10)$$
$$t_2 = t_1 * t_{1,2} \sim \mathcal{N}(5.00s, (0.235s)^2) \quad (11)$$
$$t_3 = t_2 * t_{2,3} \sim \mathcal{N}(10.18s, (0.329s)^2) \quad (12)$$
$$t_4 = t_3 * t_{3,4} \sim \mathcal{N}(11.69s, (0.336s)^2) \quad (13)$$

Fig. 3 shows histograms of the experimental transitions times from Fig. 2 compared with the analytical distributions from (10)-(13). It is clear that the analytical distributions are a good approximation to the experimental solutions. An autonomous car employing such a prediction scheme could safely continue if it intends to arrive at the roundabout at any time when the vehicle is not likely to be in state 3. This time interval can be found from (11) and (12), for example with 99% probability

$$F_{t_2}^{-1}(0.01) < t_{unsafe} < F_{t_3}^{-1}(0.99) \quad (14)$$
$$4.5s < t_{unsafe} < 10.9s \quad (15)$$

where $F_{t_i}^{-1}(P)$ is the Gaussian quantile function evaluated for the ith transition time distribution with probability P.

3. COMPLEX TEMPORAL SITUATION AWARENESS

The previous section introduced the concepts of transit and manoeuvre times for simple domains where the environment poses limits to the spatial uncertainty and prediction times are small. In less structured environments, such as those encountered by autonomous UAS, spatial uncertainty can be much larger and longer prediction horizons are often needed. Whilst the transit and manoeuvre

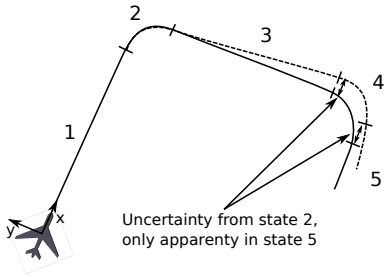

Fig. 4. Illustration of the effect of cumulative spatial uncertainty on transition time uncertainty

time distributions are still applicable for predicting the length of a particular discrete state, transitions times can no longer be found directly as the convolution of these distributions as this approach ignores the accumulation of spacial uncertainty. The following sections discuss the sources of cumulative spatial uncertainty and deals with them by including additional terms in the transition time distributions.

3.1 Sources of spatial uncertainty

Consider an aircraft conducting a series of manoeuvres, such as those undertaken in preparation for landing (McAree and Chen, 2013), illustrated in Fig. 4. As in the simple case, it is likely that manoeuvres will not be conducted perfectly, for example a pilot intending to turn through 90^o may actually stop their turn after only 85^o, as seen in state 2 of Fig. 4. This turn angle uncertainty has minimal effect on the manoeuvre time of phase 2, less than $1s$ at a typical turn rate of $6^o s^{-1}$. Likewise the length of state 3 and 4 see little effect. State 5, however, now experiences a much greater distance uncertainty due to the trajectory deviation experiences in state 3. For example, if state 3 is $2km$ long a 5^o error adds an additional $174m$ to state 5 which could take as long as $5s$ to cover.

McAree and Chen (2013) dealt with this accumulation of uncertainty by performing prediction with spatial distributions directly, with which it is then possible to calculate temporal distributions. This approach is challenging, however, as the spatial distributions are highly non-Gaussian, requiring the use of dense non-parametric distributions with high computational complexity and poor scalability. To avoid this complexity, we now consider only the accumulation in spatial uncertainty as it pertains to the calculation of temporal uncertainty.

3.2 Dealing with spatial uncertainty

Firstly, we consider the uncertainty which accumulates during a manoeuvre and then that which builds up during a subsequent transit. Finally, we must consider how to correctly apply this spatial uncertainty to our temporal distribution.

Lemma 3. Given a manoeuvre of $\bar{\psi}$ from the x axis subject to uncertainty in speed and turn rate, $v \sim \mathcal{N}(\bar{v}, \tilde{v}^2)$ and $\dot{\psi} \sim \mathcal{N}(\bar{\dot{\psi}}, \tilde{\dot{\psi}}^2)$ respectively, the subsequent spatial uncertainty in both x and y directions is

$$\begin{bmatrix}\tilde{x}^2\\ \tilde{y}^2\end{bmatrix} = \begin{bmatrix}\left(\frac{\tilde{v}}{\bar{\dot{\psi}}}\sin\bar{\psi}\right)^2 + \left(\frac{\bar{v}\tilde{\dot{\psi}}}{\bar{\dot{\psi}}^2}\sin\bar{\psi}\right)^2\\ \left(\frac{\tilde{v}}{\bar{\dot{\psi}}}(1-\cos\bar{\psi})\right)^2 + \left(\frac{\bar{v}\tilde{\dot{\psi}}}{\bar{\dot{\psi}}^2}(1-\cos\bar{\psi})\right)^2\end{bmatrix} \quad (16)$$

Proof. The nominal radius of turn is $\bar{r} = \bar{v}/\bar{\dot{\psi}}$, leading to a distance travelled in each spatial dimension (from the initiation of the manoeuvre)

$$\begin{bmatrix}\bar{x}\\ \bar{y}\end{bmatrix} = \begin{bmatrix}\frac{\bar{v}}{\bar{\dot{\psi}}}\sin\bar{\psi}\\ \frac{\bar{v}}{\bar{\dot{\psi}}}(1-\cos\bar{\psi})\end{bmatrix} \quad (17)$$

The uncertainty in radius of turn can be found from Lemma 1, assuming v and $\dot{\psi}$ are uncorrelated, as

$$\tilde{r}^2 = (\tilde{v}/\bar{\dot{\psi}})^2 + (\bar{v}\tilde{\dot{\psi}}/\bar{\dot{\psi}}^2)^2 \quad (18)$$

To correctly map the radius uncertainty to the geometry in (17), maintaining independence, each term must be transformed individually leading to (16). □

Lemma 4. Given a transit of $\bar{d}_i$ following an uncertain manoeuvre of $\psi_{i-1} \sim \mathcal{N}(\bar{\psi}_{i-1}, \tilde{\psi}^2_{i-1})$, the subsequent spatial uncertainty in both x and y directions is

$$\begin{bmatrix}\tilde{x}^2\\ \tilde{y}^2\end{bmatrix} = (\bar{d}_i\tilde{\psi}_{i-1})^2\begin{bmatrix}\cos^2(\bar{\psi}_{i-1})\\ \sin^2(\bar{\psi}_{i-1})\end{bmatrix} \quad (19)$$

assuming $\tilde{\psi}_{i-1}$ is small.

Proof. The cross track error e_{ct} associated with the uncertain manoeuvre depends on the length of the subsequent transit (Polhemus and Livingston, 1981), therefore

$$e_{ct} = \bar{d}_i\sin(\tilde{\psi}_{i-1}) \quad (20)$$

or, assuming $\tilde{\psi}_{i-1}$ is small

$$e_{ct} = \bar{d}_i\tilde{\psi}_{i-1} \quad (21)$$

This error is perpendicular to the path, therefore

$$\begin{bmatrix}e_x\\ \mathrm{e}_y\end{bmatrix} = \bar{d}_i\tilde{\psi}_{i-1}\begin{bmatrix}\cos(\bar{\psi}_{i-1})\\ \sin(\bar{\psi}_{i-1})\end{bmatrix} \quad (22)$$

To maintain positivity of the variance terms these errors are squared, leading to (19). □

The accumulation of spatial uncertainty in the x and y directions from Lemmas 3 and 4 is simply the convolution of the contribution from each state. Transforming spatial uncertainty to the temporal transition distributions is handled by convolving a distance distribution with the appropriate spatial contribution, meaning that it is only accounted during transits.

Lemma 5. Given a transit of $d_i \sim \mathcal{N}(\bar{d}_i, \tilde{d}_i^2)$ on a heading of $\bar{\psi}_i$ from the x axis and a spatial uncertainty of $(\tilde{x}_{i-1}\ \tilde{y}_{i-1})$, the distance uncertainty is updated as

$$\tilde{d}_i^{*2} = \tilde{d}_i^2 + (\tilde{x}_{i-1}\cos(\bar{\psi}_i))^2 + (\tilde{y}_{i-1}\sin(\bar{\psi}_i))^2 \quad (23)$$

and the spatial uncertainty is reduced to

$$\begin{bmatrix}\tilde{x}_i^2\\ \tilde{y}_i^2\end{bmatrix} = \begin{bmatrix}\tilde{x}_{i-1}^2(1-\cos^2(\bar{\psi}_i))\\ \tilde{y}_{i-1}^2(1-\sin^2(\bar{\psi}_i))\end{bmatrix} \quad (24)$$

Proof. We must first determine the projections of $(\tilde{x}_{i-1}\ \tilde{y}_{i-1})$ parallel to the transit, these are

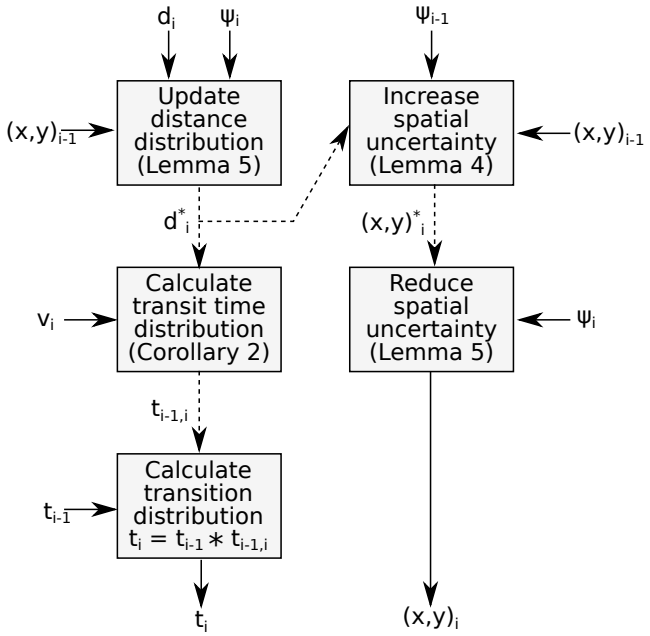

Fig. 5. Procedure for calculating transition distribution and spatial uncertainty for transits

$$\begin{bmatrix}\tilde{d}_x\\ \tilde{d}_y\end{bmatrix} = \begin{bmatrix}\tilde{x}_{i-1}\cos(\bar{\psi}_i)\\ \tilde{y}_{i-1}\sin(\bar{\psi}_i)\end{bmatrix} \quad (25)$$

The final distance distribution is the convolution of the original with these two additional variances, yielding (23). We must also reduce the spatial uncertainty by the same amount so as to avoid double accounting in future calculations, this is the deconvolution of $(\tilde{x}_{i-1}\ \tilde{y}_{i-1})$ with (25), yielding (24). □

Lemmas 3-5 provide the necessary tools to calculate complex temporal transition distributions, accounting for the accumulation of spatial uncertainty. To better understand the calculation we consider the example of an autonomous UAS approaching a busy airfield, a continuation from McAree and Chen (2013). Figs. 5 and 6 illustrate the procedure for calculating transition distributions and spatial uncertainties for transit and manoeuvre states respectively.

3.3 Autonomous unmanned aircraft example

Consider an autonomous UAS approaching a busy airfield with the intention of landing. Numerous other aircraft may be present with the same intention, and separation between aircraft is often the responsibility of the pilots. To aid safe operation in this scenario there is a predefined path which all aircraft follow, known as the traffic circuit, consisting of up to 12 discrete states (Civil Aviation Authority, 2009)

(1) *Inbound*
(2) *Deadside*
(3) *Crosswind*
(4) *Turning downwind*
(5) *Early downwind*
(6) *Mid downwind*
(7) *Late downwind*
(8) *Turning base*
(9) *Base*

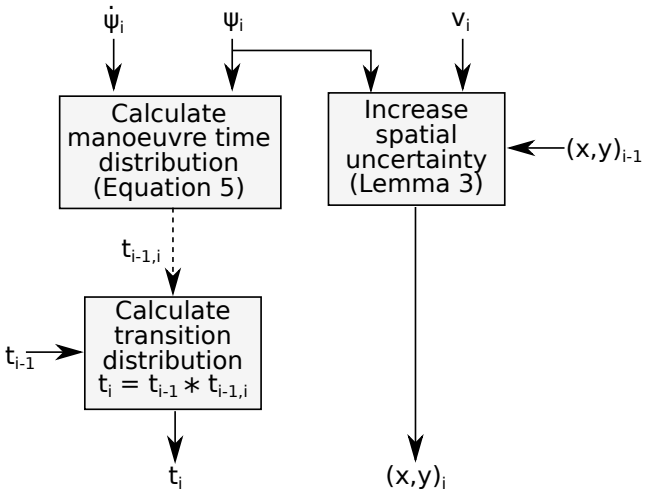

Fig. 6. Procedure for calculating transition distribution and spatial uncertainty for manoeuvres

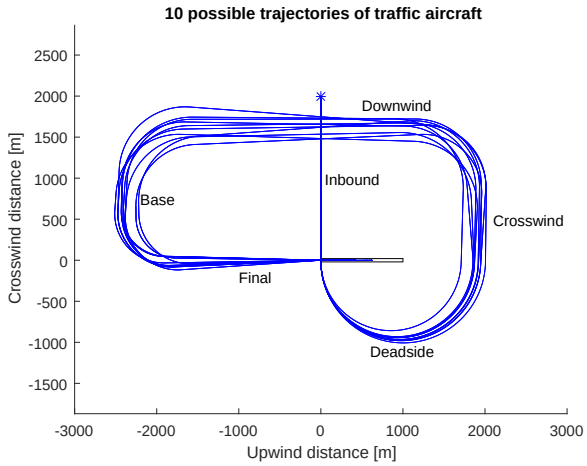

Fig. 7. 10 possible trajectories of traffic aircraft

(10) *Turning final*
(11) *Final*
(12) *On runway*

An approaching aircraft is free to join the traffic circuit at any point, provided it leaves sufficient separation to other vehicles. It is necessary, therefore, for an inbound UAS to predict the likelihood with which other aircraft will be in each state at any given future time. For this example we consider a single traffic vehicle initially located $2km$ from the airfield, intending to join via the *Deadside* state and land on the runway at the origin. Some possible two dimenionsla trajectories for the traffic vehicle are illustrated in Fig. 7.

Fig. 8 shows the calculated transition distributions for each state, in comparison with histograms from 10,000 Monte Carlo simulations. It can be seen that the analytic distributions are an excellent fit for the simulation results and can be calculated in a fraction of the time. In this example, executing on a single core of an Intel i7 4600U CPU, all analytical distributions were produced in 0.015s. Given a prediction horizon of $F^{-1}_{t_{12}}(0.99) \sim 400s$ this equates to approximately 3.75×10^{-5}s per second of prediction horizon. This represents a significant performance improvement over previously used spatial distributions which took approximately 0.21s per second of prediction horizon to calculate (McAree, 2013).

An autonomous UAS performing these predictive calculations in real time for all observed traffic vehicles would quickly build up excellent situation awareness, analogous to that of a human pilot. This artificial situation awareness can then form the basis of safe and rational route planning and decision making.

4. BAYESIAN DISCRETE TRANSITION MODELS

The previous sections have detailed the calculation of transition time distributions for future discrete states of other agents assuming their intentions are known. In many circumstances this may be the case, for example an aircraft approaching an airfield will usually broadcast its intentions to Air Traffic Control (ATC). In some cases, however, we have limited prior knowledge of the agents goals. For example, consider a similar example to that depicted in Fig. 1 but this time the observed vehicle is not signalling to turn right. It is now likely that the vehicle will continue straight on, however there is a possibility that the driver intends to turn right but has forgotten to signal.

A typical set of state transitions is shown in Fig. 9, leading to the dwell time in state 3 becoming bi-modal. Whilst we may have some prior knowledge about the transition probabilities P_4 and P_5, in general these should be learnt from observed behaviours of agents.

In addition to learning transition probabilities it is necessary for an autonomous agent to be capable of learning the parameters of its continuous mental models, such as speed and rate of turn. This requires the grouping of similar types of agents together in to classes (for example, light aircraft or commercial jets), and as not all class types may be known a-priori the agent must be capable of learning new classes from observed data.

5. CONCLUSIONS AND FUTURE WORK

This paper has presented a novel technique for the prediction of the future discrete state transitions of other agents in the environment. This prediction forms a critical part of an autonomous vehicles situation awareness, enabling it to safely plan its route through complex dynamic situations. We have presented lemmas for the prediction of how long each discrete state will last, given a mental model for the agent, and therefore at what time each state is likely to end. These predictions account for uncertainty in the mental model by treating each term as a Gaussian distribution, leading to transition times which are also Gaussian.

This paper has improved upon previous work which conducted prediction in the spatial domain by removing the need for computationally expensive non-parametric distributions. Information about how spatial uncertainty effects transition times has been retained by including additional prediction terms, without any significant increase in computational complexity. This reduction in complexity makes the prediction suitable for real time implementation and scalable to a large number of agents.

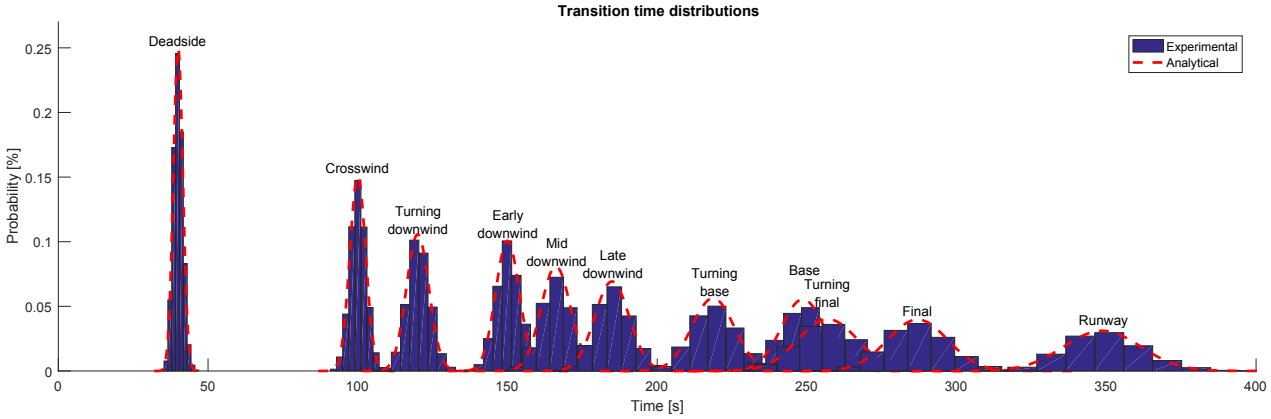

Fig. 8. Experimental and analytical transitions probabilities

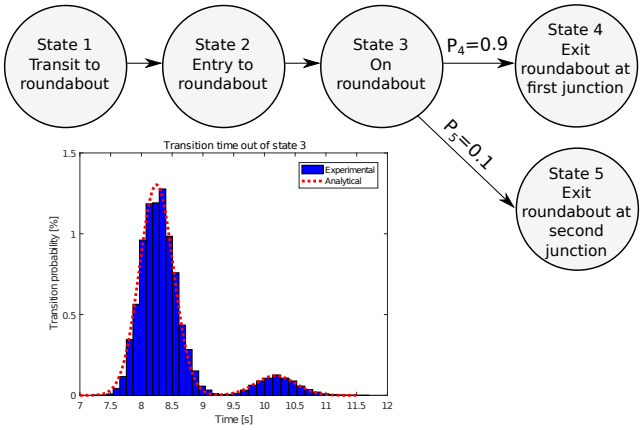

Fig. 9. Discrete transitions on roundabout if traffic does not signal

It has been shown how the prediction calculations can be applied to decision making tasks faced by both autonomous cars and UAS. Future work includes the application of this artificial situation awareness system within a decision making system, both in simulation and real world vehicles. Additionally, the learning of the requisite mental models will be investigated, both offline (from recorded data) and online (from observed behaviours). When considering online learning, verification of the produced models will be investigated to ensure future predictions remain accurate.

REFERENCES

Adams, J.A. (2007). Unmanned vehicle situation awareness: A path forward. In *Human systems integration symposium*, 31–89. Citeseer.

Bar-Shalom, Y. and Li, X.R. (1993). Estimation and tracking- principles, techniques, and software. *Norwood, MA: Artech House, Inc, 1993.*

Chen, T., Campbell, D., Gonzalez, L.F., and Coppin, G. (2015). Increasing autonomy transparency through capability communication in multiple heterogeneous uav management. In *Intelligent Robots and Systems (IROS), 2015 IEEE/RSJ International Conference on*, 2434–2439. IEEE.

Civil Aviation Authority (2009). The standard overhead join. *GA Safety Poster*, 27, 125.

Endsley, M.R. (1988). Design and evaluation for situation awareness enhancement. In *Proceedings of the Human Factors and Ergonomics Society Annual Meeting*, volume 32, 97–101. SAGE Publications.

Endsley, M.R. (1995). Toward a theory of situation awareness in dynamic systems. *Human Factors: The Journal of the Human Factors and Ergonomics Society*, 37(1), 32–64.

Hayya, J., Armstrong, D., and Gressis, N. (1975). A note on the ratio of two normally distributed variables. *Management Science*, 21(11), 1338–1341.

Hutchings, T., Jeffryes, S., and Farmer, S. (2007). Architecting uav sense & avoid systems. In *Autonomous Systems, 2007 Institution of Engineering and Technology Conference on*, 1–8. IET.

Livadas, C., Lygeros, J., and Lynch, N.A. (2000). High-level modeling and analysis of the traffic alert and collision avoidance system (tcas). *Proceedings of the IEEE*, 88(7), 926–948.

McAree, O. (2013). *Autonomous terminal area operations for unmanned aerial systems.* Ph.D. thesis, © Owen McAree.

McAree, O. and Chen, W.H. (2013). Artificial situation awareness for increased autonomy of unmanned aerial systems in the terminal area. *Journal of Intelligent & Robotic Systems*, 70(1-4), 545–555.

Pellegrini, S., Ess, A., Schindler, K., and Van Gool, L. (2009). You'll never walk alone: Modeling social behavior for multi-target tracking. In *2009 IEEE 12th International Conference on Computer Vision*, 261–268. IEEE.

Polhemus, N.W. and Livingston, D. (1981). Characterizing cross-track error distributions for continental jet routes. *Journal of Navigation*, 34(01), 134–141.

Seshadri, V. (1993). *The inverse Gaussian distribution: a case study in exponential families.* Oxford University Press.

Winfield, A.F., Blum, C., and Liu, W. (2014). Towards an ethical robot: internal models, consequences and ethical action selection. In *Conference Towards Autonomous Robotic Systems*, 85–96. Springer.